Effects of Newtonian Heating on MHD Jeffrey Hybrid Nanofluid Flow via Porous Medium

Wan Nura'in Nabilah Noranuar[1], Nor Athirah Mohd Zin[2,*], Ahmad Qushairi Mohamad[1], Lim Yeou Jiann[1], Nur Ilyana Kamis[1], Wan Faezah Wan Azmi[1], Ilyas Khan[3]

[1] Department of Mathematical Sciences, Faculty of Science, Universiti Teknologi Malaysia, 81310, Johor Bahru, Johor, Malaysia
[2] Mathematical Sciences Studies, College of Computing, Informatics and Mathematics, Universiti Teknologi MARA (UiTM), Kedah Branch, Sungai Petani Campus, 08400, Merbok, Kedah, Malaysia
[3] Department of Mathematics, College of Science Al-Zufi, Majmaah University, Al-Majmaah, 11952, Saudi Arabia

ARTICLE INFO	ABSTRACT
	In recent years, hybrid nanoparticles have gained significant attention for their ability to enhance thermal conductivity in various fluid systems, making them effective heat transport catalysts. Despite advancements in thermal fluid technology, a gap remains in understanding how hybrid nanoparticles interact within non-Newtonian Jeffrey fluid systems, particularly under complex boundary conditions like Newtonian heating. The present study aims to shed light on the effect of hybrid nanoparticles (alumina and copper) incorporated into a Jeffrey fluid model on flow and heat transport, considering them as heat transport catalyst and subject to Newtonian heating to optimize thermal efficiency. An exponentially accelerated plate is used to induce the fluid flow, taking into account the effects of porosity, MHD, and thermal radiation. The examined fluid exhibits an unsteady one-dimensional flow, formulated by deriving partial differential equations, which are subsequently transformed into ordinary differential equations using suitable non-dimensional variables and the Laplace transformation. This research distinguishes itself by presenting a novel mathematical model for MHD Jeffrey hybrid nanofluid, accounting for porosity and Newtonian heating effects. The inverse of Laplace is used to generate the exact solutions for velocity and temperature profiles, which is not explored in existing literature. Graphical representations are generated using Mathcad, depicting the velocity and temperature distributions. A comparison with prior study from the literature demonstrates strong agreement between our findings and theirs. The findings indicate that the velocity and temperature profiles of the hybrid nanofluid are higher with Newtonian heating than without it. Additionally, an increase in the Grashof number, radiation, acceleration, and porosity parameters also leads to an enhanced velocity profile.

1. Introduction

Magnetohydrodynamics (MHD) is the study of the behavior of electrically conducting fluids in the presence of a magnetic field [1]. This field combines principles from both magnetism and fluid

---

dynamics. MHD effects are commonly observed in conductive fluids such as plasmas, liquid metals, and saltwater, where the interaction between fluid motion, magnetic fields, and heat transfer governs the system's behavior [2]. In nuclear reactors, magnetic fields are used to control liquid metal coolant flow, while in fusion reactors, they manage plasma motion and heat during energy generation. In medicine, MHD techniques are employed to guide magnetized particles for targeted drug delivery, influencing drug release through controlled heat transfer. Given the significance of MHD effects, many researchers have studied their unique impact on fluid flow. Ali *et al.,* [3] investigated the dynamics of Casson fluid flow in MHD systems with thermal radiation and heat sink effects. Sehra *et al.,* [4] examined heat transfer and MHD effects in second-grade fluids, with a focus on the emerging field of fractional derivatives in fluid dynamics. Noranuar *et al.,* [5] studied the non-coaxial rotating MHD flow of a viscous fluid, exploring the physical interaction of magnetic fields with rotating flow. Ramzan *et al.,* [6] analytically studied heat and mass transfer in Casson fluid flow under the influence of a magnetic field, obtaining solutions using the Laplace transform method. In certain cases, such as MHD flow through porous media, heat transfer characteristics are further altered. The ability to control fluid flow and heat transfer in porous media using magnetic fields has significant applications, ranging from energy systems and oil extraction to biomedical devices and advanced cooling systems. Understanding the interaction between MHD effects and porous media is essential for optimizing the performance and efficiency of these systems. Due to the complex and intriguing behavior of MHD flow through porous media, this topic continues to attract attention from researchers [7-9]. Recently, Noranuar *et al.,* [10] explored the behavior of Casson fluid flow in a channel with heat and mass transfer. Haq *et al.,* [11] investigated unsteady MHD viscous fluid flow through a porous medium, confined by a cosine and sine oscillating plate. Abbas *et al.,* [12] discussed the influence of porosity and MHD on Casson fluid flow over an accelerated porous plate. While the application of a magnetic field typically retards fluid flow, which can be disadvantageous in processes like cooling systems where rapid fluid movement is needed, interacting MHD flow within a porous medium can enhance fluid control and stability, providing benefits for applications such as filtration or petroleum extraction.

Newtonian heating refers to a boundary condition where the heat flux is proportional to the difference between the surface and the ambient fluid temperatures [13]. This is significant in systems where heat generation or absorption is continuously influenced by the changing temperatures of both the surface and fluid, such as in heat exchangers, cooling systems, or thermal management processes in electronics [14]. The impact of Newtonian heating on fluid dynamics and heat transfer processes is evident in different models. Studies have shown that Newtonian heating tends to enhance temperature profiles while affecting fluid velocity differently based on the specific fluid model and boundary conditions [15]. The investigation of Jeffrey fluid flow with Newtonian heating effects was conducted by Riaz *et al.,* [16], considering fluid flow induced by a moving plate. Mohd Zin *et al.,* [17] scrutinized the impacts of Newtonian heating on Jeffrey fluid flow across an oscillating plate in the presence of heat and mass transfer. Ramzan *et al.,* [18] used a moving plate to initiate the Jeffrey fluid flow and introduced the effects of Newtonian heating and thermal radiation on heat transfer. Anwar *et al.,* [19] applied ramped velocity conditions and Newtonian heating to investigate the motion of Jeffrey fluid near a vertical plate. Despite many studies focusing on constant boundary conditions, adding complex conditions like Newtonian heating can improve simulations. Newtonian heating provides a more accurate representation of heat transfer, leading to better predictions of temperature and system performance.

The Jeffrey fluid model is a mathematical representation used in fluid dynamics to describe the behavior of non-Newtonian fluids. Non-Newtonian fluids are those whose viscosity is not constant and varies with the rate of shear strain. Compared to other viscoelastic flow models, the Jeffrey fluid

model is simpler. Its equations can be reduced to those of Newtonian models, making it a generalization of the commonly used Newtonian fluid model [20]. Unlike standard viscous fluid models, the Jeffrey fluid model can capture the stress relaxation behavior of non-Newtonian fluids. It effectively describes a category of non-Newtonian fluids characterized by a unique memory time scale, known as the relaxation time [21]. Concerning the Jeffrey fluid model, Zin *et al.,* [22] addressed the analytical solutions for heat transfer and rotating fluid flow incorporating the magnetic field, porosity, and radiation effects. The study was extended by Hari Babu *et al.,* [23], imposing the Hall and ion-slip effect and was also extended by Krishna [24], considering ramped wall velocity and temperature effects. A generalized heat transfer for Jeffrey fluid flow was examined by Asjad *et al.,* [25] and was further extended by Bajwa *et al.,* [26], considering the fluid moving through a porous medium with magnetic field effects and exponentially accelerating plate. Another study of Jeffrey fluid flow was conducted by Aleem *et al.,* [27], considering the investigated flow within a moving channel, and was also performed by Siddique *et al.,* [28], introducing the effect of heat absorption on thermal transport, which directly affects velocity distribution.

In contemporary engineering and scientific endeavors, there is a concerted effort to improve transport processes across various systems, such as heat exchangers, electronic devices, and chemical reactors. This improvement can involve modifying different elements within these systems, such as heat transfer surfaces or the working fluid. Nanofluids, which are base fluids infused with solid material nanoparticles, represent effective working fluids applicable across diverse engineering systems [29-32]. Combining two or more different nanoadditives with the base fluid leads to the creation of hybrid nanofluids [33]. Hybrid nanofluids offer advantages such as increased thermal conductivity, improved heat absorption, and enhanced energy transport efficiency compared to traditional heat transfer fluids [34]. Eshgarf *et al.,* [35] have extensively detailed the preparation of hybrid nanofluids, including their advantages and drawbacks. The primary objective in such endeavors is to analyze the behavior of hybrid nanofluids within different systems. Numerous researchers have contributed valuable insights into this area. Saqib *et al.,* [36] investigated analytically the behavior of Brinkman hybrid nanofluid flowing through two parallel plates, where both plates are at rest. Ikram *et al.,* [37] extended the study of Saqib *et al.,* [36] by introducing the effect of magnetic field in fluid flow. Roy *et al.,* [38] modelled the unsteady flow of water hybrid nanofluid using copper and alumina particles over an oscillating plate. Elelamy [39] used Casson fluid model to investigate analytically the bio-heat transfer and hybrid nanofluid flow within a channel with magnetic field and porosity effects. Rajesh *et al.,* [40] applied the method of Laplace transformation to provide the analytical solution for the unsteady flow of hybrid nanofluid past an exponentially accelerated plate. Anwar *et al.,* [41] examined analytically the mixed convection of Casson hybrid nanofluids flow through a moving channel, where the fluid flow is also affected by the thermal radiation. Ali *et al.,* [42] provided an analytical solution for the flow of Maxwell hybrid nanofluid in a stationary channel using Laplace transformation.

Based on the review, the interaction between MHD and porosity effects has not been thoroughly explored in hybrid nanofluid flow studies. Inspired by Zin *et al.,* [43], who investigated MHD hybrid nanofluid flow using the Jeffrey fluid model without considering porosity effects, this present study aims to address that gap by examining heat transfer in MHD Jeffrey hybrid nanofluid flow through a porous medium. While previous research involving models such as the Brinkman and Casson fluid models has provided valuable insights into fluid dynamics, these models are limited in their ability to fully capture the unique viscoelastic properties and relaxation times characteristic of real-world fluids. The Jeffrey model, on the other hand, is well-suited for analyzing viscoelastic fluids as it accounts for both the elastic behavior of the fluid and its ability to flow under stress. Additionally, motivated by previous research on the influence of Newtonian heating in Jeffrey fluid flow, this

present study incorporates the effect of Newtonian heating into the analysis. Investigating the impact of Newtonian heating on Jeffrey hybrid nanofluid flow is essential for enhancing heat transfer in real-world applications, such as electronics cooling, bioengineering (e.g., hyperthermia treatments), and chemical reactors, where precise thermal control is critical. Understanding this combination can help optimize thermal management in complex systems, improving both the efficiency and stability of these technologies.

Furthermore, it is worth noting that the studies mentioned earlier used the Laplace transform method to obtain analytical solutions for their respective problems. According to Wang *et al.,* [44], the Laplace transform method offers several advantages in problem-solving, including its role in superposing solutions and efficiently deriving exact solutions for transient problems with varying boundary conditions. These analytical solutions help validate numerical methods, enhance the understanding of physical mechanisms, and provide insights into complex phenomena such as porous media flow and nanoparticle transport [45]. Additionally, analytical solutions allow for rapid estimation and comprehension of behaviors, supporting engineering applications and numerical verification, while reducing computational costs and instrumentation needs in navigation problems by offering functional dependencies for geodesic lines [46]. Considering these benefits, the present study focuses on the analytical investigation of heat transfer in convective Jeffrey hybrid nanofluid flow, accounting for Newtonian heating. The hybrid nanofluid is assumed to flow through a porous medium under the influence of a magnetic field, incorporating both porosity and MHD effects. The problem is modeled with an exponentially accelerated plate, and the Laplace transform technique is applied to derive the analytical solution for the velocity and temperature of the Jeffrey hybrid nanofluid.

2. Mathematical Formulation

The mathematical model unveils the thermal properties of an electrically conducting Jeffrey hybrid nanofluid induced magnetohydrodynamic (MHD) flow over an accelerated vertical plate through a porous medium as illustrated in Figure 1. This plate accelerates exponentially with velocity $u = u_0 \exp(at)$, prompts motion of hybrid nanofluid over the plate with a Newtonian heating and radiation effect. The model is formulated within the specified flow constraints:

i) Unsteady flow and incompressible Jeffrey hybrid nanofluid flow.
ii) Uniform transverse magnetic field with strength of B_0 is applied, hence inducing the MHD effect.
iii) At $t = 0$, both plate and fluid are motionless at a constant temperature of free stream, T_∞. When $t > 0$, the plate starts to accelerate exponentially while the temperature is changed to a constant temperature of T_w, inducing the flow of Jeffrey hybrid nanofluid.
iv) The hybrid nanofluid is assumed to flow through a porous medium.
v) The radiative phenomenon is utilized in energy equation and Newtonian heating is imposed at its boundary conditions.
vi) The nanoparticles are constrained to maintain a spherical shape and uniform size. Both nanoparticles and base fluid are assumed to be in stable state, moving at the same velocity.

According to the constraints, the modelled problem is governed by the subsequent set of equations [17,22]:

$$\rho_{hnf}\frac{\partial u}{\partial t} = \frac{\mu_{hnf}}{1+\lambda_1}(1+\lambda_2)\frac{\partial^2 u}{\partial y^2} - \frac{\mu_{hnf}}{k^*(1+\lambda_1)}\left(1+\lambda_2\frac{\partial}{\partial t}\right)u - \sigma B_0^2 u + g(\rho\beta_T)_{hnf}(T - T_\infty),$$ (1)

$$\left(\rho C_p\right)_{hnf}\frac{\partial T}{\partial t} = k_{hnf}\frac{\partial^2 T}{\partial y^2} - \frac{\partial q_r}{\partial y},$$ (2)
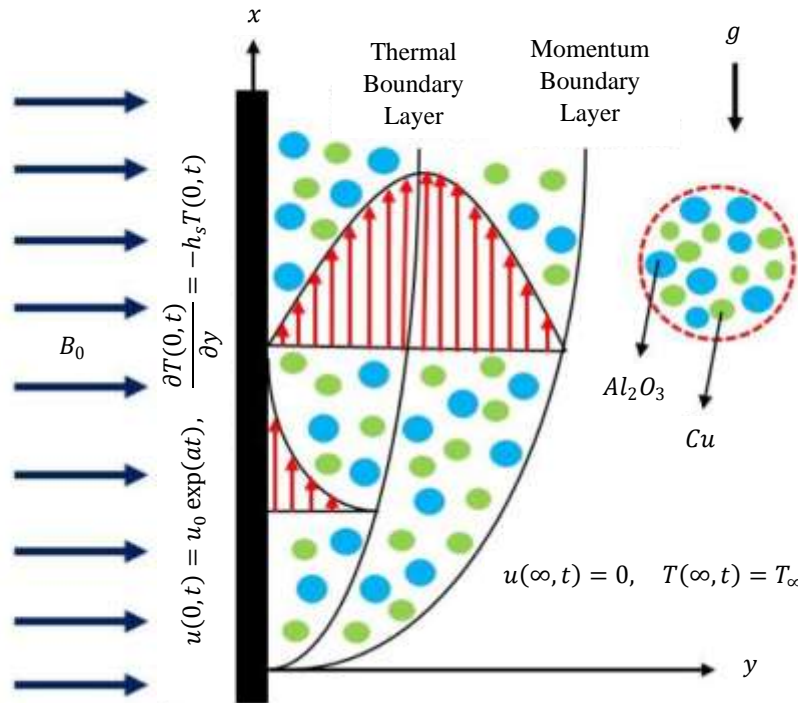

Fig. 1. Physical model of the problem

subjected to initial and boundary conditions as [17, 40]

$$u(y,0) = 0, \quad T(y,0) = T_\infty; \quad y > 0,$$ (3)

$$u(0,t) = u_o \exp(at), \quad \frac{\partial T(0,t)}{\partial y} = -h_s T(0,t); \quad t > 0,$$ (4)

$$u(\infty,t) = 0, \quad T(\infty,t) = T_\infty; \quad t > 0,$$ (5)

with ratio of relaxation time and retardation time (λ_1), retardation time (λ_2), density (ρ), dynamic viscosity (μ), permeability of medium (k^*), electrical conductivity (σ), acceleration due to gravity (g), thermal expansion coefficient (β_T), heat capacitance (C_p), thermal conductivity (k), and radiative heat flux (q_r). In addition, the subscription of hnf denotes hybrid nanofluid where its correlation is mathematically given as [36,37]

$$\phi_{hnf} = \phi_1 + \phi_2, \quad \rho_{hnf} = \phi_1\rho_1 + \phi_2\rho_2 + (1-\phi_{hnf})\rho_f, \quad \mu_{hnf} = \frac{\mu_f}{(1-\phi_1-\phi_2)^{2.5}},$$

$$(\rho\beta_T)_{hnf} = \phi_1(\rho\beta_T)_1 + \phi_2(\rho\beta_T)_2 + (1-\phi_{hnf})(\rho\beta_T)_f,$$

$$\left(\rho C_p\right)_{hnf} = \phi_1\left(\rho C_p\right)_1 + \phi_2\left(\rho C_p\right)_2 + (1-\phi_{hnf})\left(\rho C_p\right)_f,$$

$$\frac{k_{hnf}}{k_f} = \frac{(k_{hp}+2k_f)-2\phi_{hnf}(k_f-k_{hnp})}{(k_{hp}+2k_f)+\phi_{hnf}(k_f-k_{hnp})}, \quad k_{hp} = \frac{\phi_1 k_1 + \phi_2 k_2}{\phi_1 + \phi_2},$$ (6)

with the subscription $f, 1$, and 2 referred as base fluid, Alumina (Al_2O_3), and Copper (Cu) nanoparticles, respectively. Eq. (6) is utilized throughout the calculation by referring to the thermophysical properties in Table 1.

Table 1
Thermophysical properties of hybrid nanofluids [22,40]

Physical properties	Nanoparticles		Base fluid		
	Al_2O_3	Cu	Water	Kerosene	Ethylene glycol
ρ (kg/m^3)	3970	8933	997.1	780	1115
C_p (J/kgK)	765	385	4179	2090	2386
k (W/mK)	40	401	0.613	0.149	0.2499
β (K^{-1})	0.85×10^{-5}	1.67×10^{-5}	21×10^{-5}	9.9×10^{-4}	3.41×10^{-3}
Pr	-	-	6.2	21	203

Making use of the Rosseland approximation provides the following expression of radiative heat flux (q_r) [40].

$$q_r = -\frac{4\sigma_s}{3k_e}\frac{\partial T^4}{\partial y}, \tag{7}$$

where k_e is the coefficient of Rosseland absorption and σ_s is Stehfan-Boltzmann constant, respectively. It is important to highlight that through the utilization of the Rosseland approximation, our scope is limited to optically thick nanofluids. If temperature fluctuations within the flow are sufficiently minor to express T^4 as a linear function of temperature, then the Taylor series expansion for T^4 around T^∞ as follows, disregarding higher-order expressions:

$$T^4 \cong 4T_\infty^3 T - 3T_\infty^4. \tag{8}$$

Considering Eq. (7) and (8), Eq. (2) is simplified to [40],

$$\frac{\partial T}{\partial t} = \frac{k_f}{(\rho C_p)_{hnf}}\left(\frac{k_{hnf}}{k_f} + \frac{16\sigma_s T_\infty^3}{3k_f k_e}\right)\frac{\partial^2 T}{\partial y^2}. \tag{9}$$

The following non-dimensional quantities are substituted [22]

$$u^* = \frac{u}{u_0}, \quad t^* = \frac{tu_0^2}{v_f}, \quad y^* = \frac{yu_0}{v_f}, \quad T^* = \frac{T-T_\infty}{T_\infty}, \tag{10}$$

into Eq. (1), Eq. (3) to (5), and Eq. (9). Then, incorporating Eq. (6) give the following equations (the $*$ sign is dropped for simplicity)

$$A_0\frac{\partial u}{\partial t} = \left(\frac{A_1}{1+\lambda_1}\right)\frac{\partial^2 u}{\partial y^2} + \left(\frac{A_1\lambda}{1+\lambda_1}\right)\frac{\partial^3 u}{\partial y^2 \partial t} - Du + A_2 GrT, \tag{11}$$

$$\frac{\partial T}{\partial t} = \frac{1}{B_3}\frac{\partial^2 T}{\partial y^2}, \tag{12}$$

associated with dimensionless conditions

$$u(y,0) = 0, \quad T(y,0) = 0; \quad y > 0, \tag{13}$$

$$u(0,t) = \exp(at), \quad \frac{\partial T(0,t)}{\partial y} = -\gamma\big(1 + T(0,t)\big); \quad t > 0, \tag{14}$$

$$u(\infty,t) = 0, \quad T(\infty,0) = 0; \quad t > 0, \tag{15}$$

where

$$A_0 = \left(\frac{\phi_1 \rho_1 + \phi_2 \rho_2}{\rho_f}\right) + (1 - \phi_{hnf}), \quad A_1 = \frac{1}{(1-\phi_1-\phi_2)^{2.5}},$$
$$A_2 = \frac{\phi_1 (\rho\beta_T)_1}{(\rho\beta_T)_f} + \frac{\phi_2 (\rho\beta_T)_2}{(\rho\beta_T)_f} + (1 - \phi_{hnf}), \quad D = M + \frac{A_1}{K},$$
$$B_1 = \frac{\phi_1 (\rho C_p)_1 + \phi_2 (\rho C_p)_2}{(\rho C_p)_f} + (1 - \phi_1 - \phi_2), \quad B_2 = \frac{k_{khnf}}{k_f} + Rd, \quad B_3 = \frac{\mathrm{Pr} B_1}{B_2}, \tag{16}$$

are arbitrary constants while

$$\lambda = \frac{\lambda_2 u_0^2}{v_f}, \quad M = \frac{v_f \sigma B_0^2}{\rho_f u_0^2}, \quad \frac{1}{K} = \frac{v_f^2}{u_0^2 k}, \quad Gr = \frac{g(\beta_T v)_f T_\infty}{u_0^3}, \quad Rd = \frac{16 \sigma_s T_\infty^3}{3 k_f k_e}, \quad \mathrm{Pr} = \frac{v_f}{\alpha_f}, \quad a = \frac{av}{u_0^2}, \tag{17}$$

are dimensionless Jeffrey parameter (λ), magnetic field parameter (M), porosity parameter (K), Grashof number (Gr), radiation parameter (Rd), Prandtl number (Pr), and acceleration parameter (a) with their physical meaning is explained in Table 2.

3. Solution by Laplace Transformation

A flowchart summarizing the stepwise process for calculating the analytical solutions is provided in Figure 2 to facilitate a clearer understanding of the methodology.
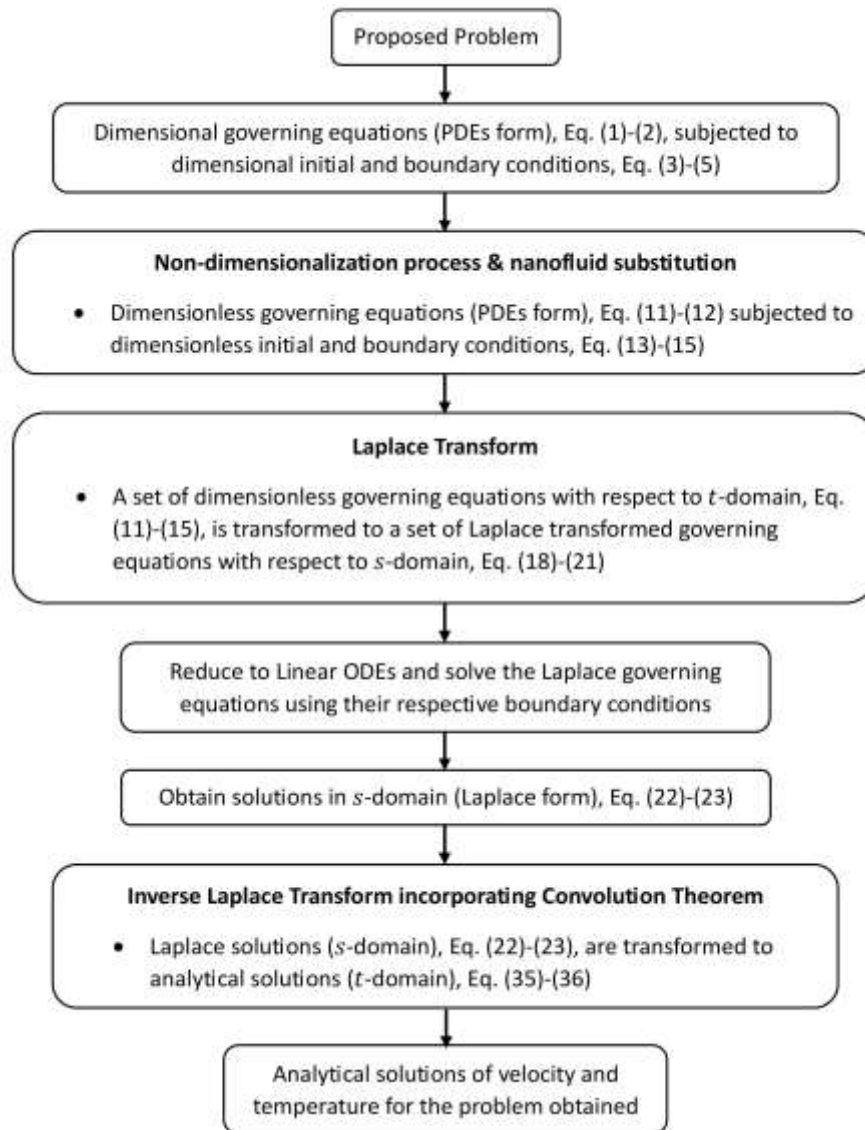
Fig. 2. Methodology flowchart

Table 2
Physical meaning of parameters

Parameter	Physical meaning
Jeffrey parameter, λ	The parameter associates to Jeffrey fluid model and describes a non-Newtonian fluid behavior, capturing both viscous and elastic properties.
Magnetic field parameter, M	The interaction of electrically conducting fluid moving in the magnetic field.
Porosity parameter, K	The fraction of void (empty) space in a material compared to its total volume
Grashof number, Gr	The ratio of buoyancy forces (which cause fluid motion) to viscous forces (which resist fluid motion).
Radiation parameter, Rd	The parameter associates to heat transfer that involves the emission and propagation of energy in the form of electromagnetic waves.
Prandtl number, Pr	The ratio of momentum diffusivity to thermal diffusivity
Acceleration parameter, a	The parameter associates to the movement of plate to initiate the fluid flow.

Here, the Laplace transform is applied on Eq. (11) to (15), giving the following expression of ordinary differential equations (ODEs).

$$A_0 s\bar{u}(y,s) = \left(\frac{A_1}{1+\lambda_1}\right)\frac{d^2\bar{u}(y,s)}{dy^2} + \left(\frac{\lambda A_1}{1+\lambda_1}\right)s\frac{d^2\bar{u}(y,s)}{dy^2} - D\bar{u}(y,s) + A_2 Gr\bar{T}(y,s),$$ (18)

$$\frac{d^2\bar{T}(y,s)}{dy^2} - B_3 s\bar{T}(y,s) = 0,$$ (19)

subjected to transformed conditions

$$\bar{u}(0,s) = \frac{1}{s-a}, \quad \bar{u}(\infty,s) = 0; \quad s > 0,$$ (20)

$$\frac{d\bar{T}(0,s)}{dy} = -\gamma\left(\frac{1}{s} + \bar{T}(0,s)\right), \quad \bar{T}(\infty,s) = 0; \quad s > 0.$$ (21)

At this part, $\bar{u}(y,s)$ and $\bar{T}(y,s)$ represent the Laplace transform of $u(y,t)$ and $T(y,t)$. Next, Eq. (20) and (21) are used to obtain the Laplace solution of Eq. (18) and (19) as

$$\bar{u}(y,s) = \bar{u}_1(y,s) + \frac{a_1 B_4}{a_2}\bar{u}_2(y,s) - \frac{a_1}{a_2}\bar{u}_3(y,s),$$ (22)

$$\bar{T}(y,s) = \frac{B_4}{s(\sqrt{s}-B_4)}\exp\left(-y\sqrt{B_3 s}\right),$$ (23)

where

$$\bar{u}_1(y,s) = \left(\frac{1}{s-a}\right)\exp\left(-y\sqrt{a_0\left(\frac{D+A_0 s}{1+\lambda s}\right)}\right),$$ (24)

$$\bar{u}_2(y,s) = \left(\frac{1}{s(\sqrt{s}-B_4)}\right)\left(\frac{1}{(s+b_0)^2-b_1}\right)\exp\left(-y\sqrt{a_0\left(\frac{D+A_0 s}{1+\lambda s}\right)}\right),$$ (25)

$$\bar{u}_3(y,s) = \left(\frac{B_4}{s(\sqrt{s}-B_4)}\right)\left(\frac{1}{(s+b_0)^2-b_1}\right)\exp\left(-y\sqrt{B_3 s}\right),$$ (26)

In Eq. (22) to (26), $a_0, a_1, a_2, B_4, b_0,$ and b_1 are the arbitrary constant written as

$$a_0 = \frac{1+\lambda_1}{A_1}, \quad a_1 = (1+\lambda_1)\frac{A_2 Gr}{A_1}, \quad a_2 = B_3\lambda, \quad B_4 = \frac{\gamma}{\sqrt{B_3}}, \quad b_0 = \frac{a_5}{2}, \quad b_1 = \frac{a_5^2 - 4a_6}{4},$$ (27)

where

$$a_5 = \frac{a_3}{a_2}, \quad a_6 = \frac{a_4}{a_2}, \quad a_3 = B_3 + a_0 A_0, \quad a_4 = a_0 D.$$ (28)

Since Laplace solutions in Eq. (24) to (26) involves the product of two and three functions, therefore the inverse Laplace transform will be needed to use the convolution theorem. To employ the inverse Laplace transform, Eq. (24) to (26) is set up in the form

$$\bar{u}_1(y,s) = \bar{u}_{11}(s) \cdot \bar{u}_{12}(y,s),$$ (29)

$$\bar{u}_2(y,s) = \bar{u}_{21}(s) \cdot [\bar{u}_{22}(s) \cdot \bar{u}_{12}(y,s)], \tag{30}$$

$$\bar{u}_3(y,s) = \bar{u}_{22}(s) \cdot \bar{u}_{31}(y,s), \tag{31}$$

where

$$\bar{u}_{11}(s) = \left(\frac{1}{s-a}\right), \quad \bar{u}_{12}(y,s) = \exp\left(-y\sqrt{a_0\left(\frac{D+A_0 s}{1+\lambda s}\right)}\right), \tag{32}$$

$$\bar{u}_{21}(s) = \left(\frac{1}{s(\sqrt{s}-B_4)}\right), \quad \bar{u}_{22}(s) = \left(\frac{1}{(s+b_0)^2-b_1}\right), \tag{33}$$

$$\bar{u}_{31}(y,s) = \left(\frac{B_4}{s(\sqrt{s}-B_4)}\right)\exp\left(-y\sqrt{B_3 s}\right) = \bar{T}(y,s). \tag{34}$$

Employing the inverse Laplace on Eq. (22) to (23) and Eq. (32) to (34) gives

$$u(y,t) = u_1(y,s) + \frac{a_1 B_4}{a_2} u_2(y,s) - \frac{a_1}{a_2} u_3(y,s), \tag{35}$$

$$T(y,t) = \exp\left(B_4^2 t - y B_4\sqrt{B_3}\right)\operatorname{erfc}\left(\frac{y}{2}\sqrt{\frac{B_3}{t}} - B_4\sqrt{t}\right) - \operatorname{erfc}\left(\frac{y}{2}\sqrt{\frac{B_3}{t}}\right). \tag{36}$$

where

$$u_{11}(t) = \exp(at), \tag{37}$$

$$u_{12}(y,t) = \delta(t)\exp\left(-y\sqrt{d_0}\right) + \int_0^\infty \frac{y}{2u}\sqrt{\frac{d_1}{\pi t}}\exp\left(-\frac{y^2}{4u} - ud_0 - \frac{t}{\lambda}\right)\cdot I_1\left(2\sqrt{ud_1 t}\right)du, \tag{38}$$

$$u_{21}(t) = -\frac{1}{B_4}\left[1 - \exp(B_4^2 t)\operatorname{erfc}\left(-B_4\sqrt{t}\right)\right], \tag{39}$$

$$u_{22}(t) = \frac{1}{\sqrt{b_1}}\exp(-b_0 t)\sinh\left(\sqrt{b_1} t\right), \tag{40}$$

$$u_{31}(y,t) = T(y,t), \tag{41}$$

with

$$d_0 = \frac{a_0 A_0}{\lambda}, \quad d_1 = \frac{a_0 A_0}{\lambda^2} - \frac{a_0 D}{\lambda}. \tag{42}$$

Then, the solution of $u_1(y,t), u_2(y,t)$ and $u_3(y,t)$ are obtained by applying the convolution theorem, which finally give

$$u_1(y,t) = \exp\left(at - y\sqrt{d_0}\right) + \int_0^t \int_0^\infty \frac{y}{2u}\sqrt{\frac{d_1}{\pi q}}\exp\left(a(t-q) - \frac{y^2}{4u} - ud_0 - \frac{q}{\lambda}\right) I_1\left(2\sqrt{ud_1 q}\right)du\,dq \tag{43}$$

$$u_2(y,t) = \int_0^t \int_0^p \int_0^\infty \begin{bmatrix} \frac{1}{\sqrt{b_1}} \int_0^t \left[\exp\left(B_4^2(t-p) - b_0 p - y\sqrt{d_0}\right) \operatorname{erfc}\left(-B_4\sqrt{t-p}\right) - 1 \right] \sinh\left(p\sqrt{b_1}\right) dp + \\ \frac{y}{2u} \sqrt{\frac{d_1}{\pi b_1 q}} \left[\exp\left(B_4^2(t-p)\right) \operatorname{erfc}\left(-B_4\sqrt{t-p}\right) - 1 \right] \times \\ \exp\left(-\frac{y^2}{4u} - ud_0 - b_0(p-q) - \frac{q}{\lambda}\right) \sinh\left(\sqrt{b_1(p-q)}\right) I_1\left(2\sqrt{ud_1 q}\right) \end{bmatrix} du\,dq\,dp$$

(44)

$$u_3(y,t) = \frac{1}{\sqrt{b_1}} \int_0^t \begin{bmatrix} \exp\left(b_0(t-q)\right) \sinh\left(\sqrt{b_1}(t-q)\right) \times \\ \exp\left(B_4^2 q - yB_4\sqrt{B_3}\right) \operatorname{erfc}\left(\frac{y}{2}\sqrt{\frac{B_3}{q}} - B_4\sqrt{q}\right) - \operatorname{erfc}\left(\frac{y}{2}\sqrt{\frac{B_3}{q}}\right) \end{bmatrix} dq$$

(45)

4. Results and Discussion

In this section, graphical illustrations of the analytical solutions in Eq. (35) and (36) incorporating Eq. (43) to (45), are generated using Mathcad software in accordance with the thermophysical properties in Table 1. Further analysis on the velocity and temperature of Jeffery hybrid nanofluid is conducted by assigning the parameter values as $\gamma = 0.5, \lambda_1 = 1, \lambda = 1, M = 2, K = 2, Rd = 0.5, a = 1$, and $Gr = 2$.

4.1 Verification of Results

The accuracy of the derived solution is confirmed by comparing the solutions in Eq. (35) and (36) with those obtained by Zin *et al.,* [17]. This comparison is carried out by setting the nanoparticle volume fraction and acceleration parameter in the present study to zero ($\phi_1 = 0, \phi_2 = 0, a = 0$), and allowing the porosity parameter to approach infinity ($K \to \infty$). Meanwhile, for the study by Zin *et al.,* [17], the modified Grashof number, Schmidt number, and phase angle are assigned to zero ($Gm = Sc = \omega t = 0$). The comparison reveals that the velocity and temperature profiles obtained from both the current study and the previous work are indistinguishable, as clearly illustrated in Figure 3 and 4. This alignment demonstrates that the accuracy of the obtained solutions has been verified and is in excellent agreement.
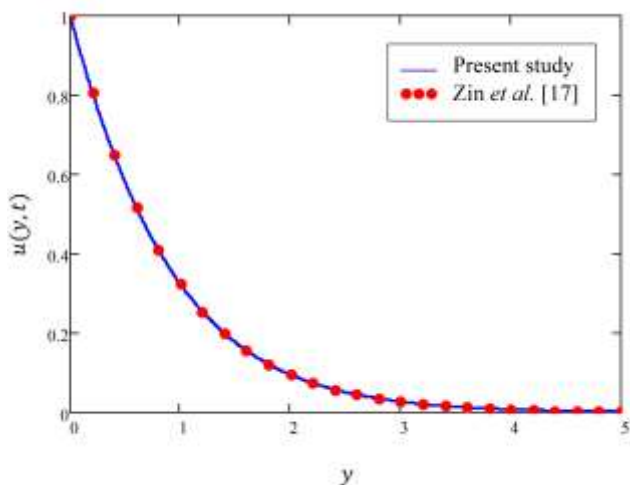

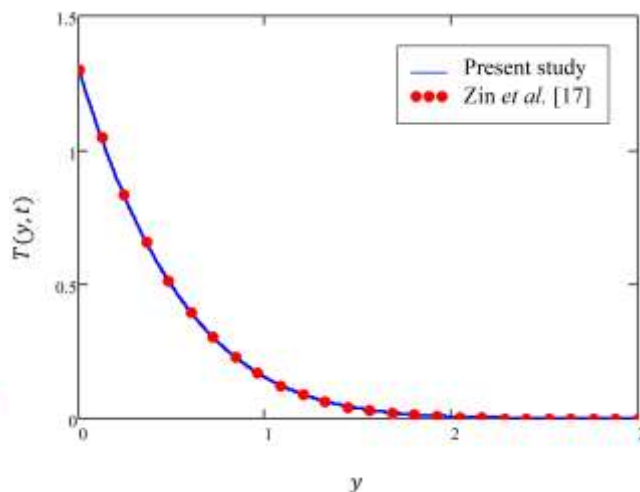**Fig. 3.** Verification of velocity profile, $u(y,t)$

Fig. 4. Verification of temperature profile, $T(y,t)$

4.2 Velocity Profiles

Figure 5 displays the velocity profile of a hybrid nanofluid affected by the material parameter, λ_1 of the Jeffrey fluid. While the velocity profile exhibits insignificant alterations with increasing λ_1 values, noticeable increments can be observed upon closer examination within the zoomed-in region. Figure 6 illustrates that an augmentation in λ has a tendency to slow down the fluid motion. This phenomenon can be explained by the fact that λ represents the Jeffrey (viscoelastic) parameter, signifying the material's combined elastic and viscous behavior during deformation. Consequently, increases in viscosity and elasticity consistently oppose the fluid velocity. Changes in the viscoelastic parameter, λ have important implications for engineering systems where fluid flow is crucial. For example, in heat exchangers, a higher λ value slows fluid motion, diminishing heat transfer efficiency and potentially requiring adjustments in flow rates or fluid composition. In biomedical devices, such as blood pumps, increased viscoelasticity could hinder fluid flow, necessitating design modifications to ensure proper circulation without compromising performance.
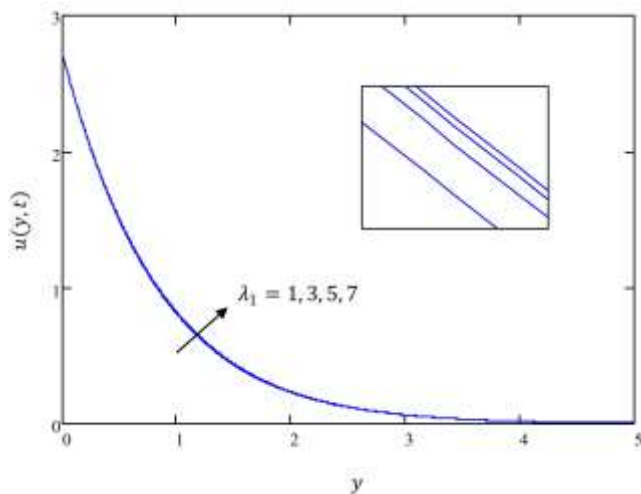

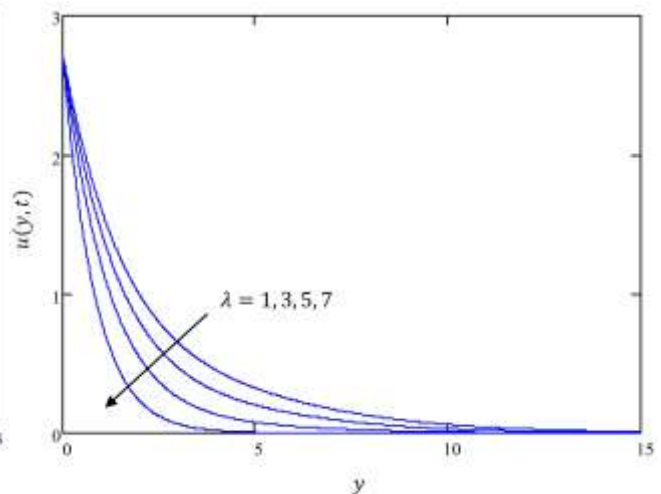**Fig. 5.** Jeffrey hybrid nanofluid velocity, $u(y,t)$ vs material parameter, λ_1

Fig. 6. Jeffrey hybrid nanofluid velocity, $u(y,t)$ vs Jeffrey parameter, λ

The effect of Al_2O_3 volume fraction, ϕ_1 and Cu volume fraction, ϕ_2 on the nanofluid velocity profiles are illustrated in Figure 7 and 8. In these figures, increasing the volume fraction of both nanoparticles results in a diminution of the velocity profiles. This situation reflects the fact that nanoparticles in the fluid introduce additional obstacles to the flow, effectively increasing the fluid's viscosity. As the volume fraction of nanoparticles rises, the viscosity of the nanofluid increases accordingly. Higher viscosity results in greater resistance to flow, slowing down fluid particles and leading to a decrease in the velocity profile. The same physical behavior is exhibited for the increasing volume fraction of hybrid nanofluid, ϕ_{hnf}, where the reduction in velocity is reported as shown in Figure 9. This impact is analyzed by choosing water as the base fluid. This situation is due to the same reason as explained for the impact of ϕ_1 and ϕ_2. Physically, changes in ϕ_1 and ϕ_2 values will subsequently alter the overall value of ϕ_{hnf}, where its relation is stated in Eq. (6). Increasing values of ϕ_1 or ϕ_2 directly imply an increase in the ϕ_{hnf} value. Hence, a greater value of ϕ_{hnf} leads to the thickening of the fluid (making it more viscous) and consequently retards the velocity profiles. In biomedical devices, such as drug delivery systems or microfluidic pumps, higher ϕ_{hnf} can slow fluid flow, affecting precise control. Adjustments in nanoparticle concentration are necessary to maintain

efficiency and fluid dynamics, emphasizing the importance of fine-tuning ϕ_{hnf} in various applications.
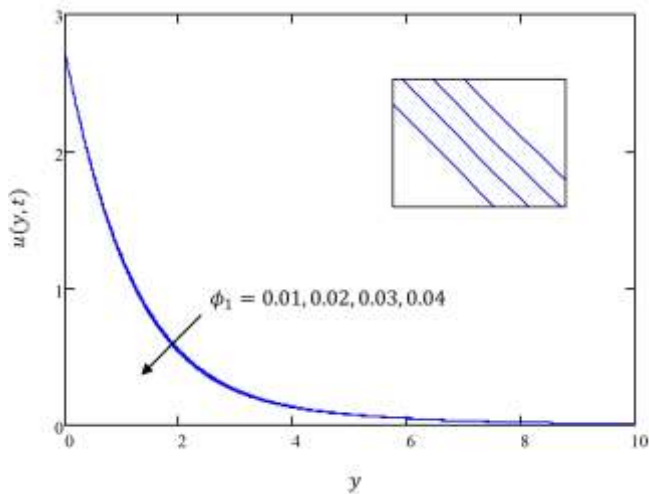

Fig. 7. Jeffrey hybrid nanofluid velocity, $u(y,t)$ vs volume fraction of Al_2O_3, ϕ_1
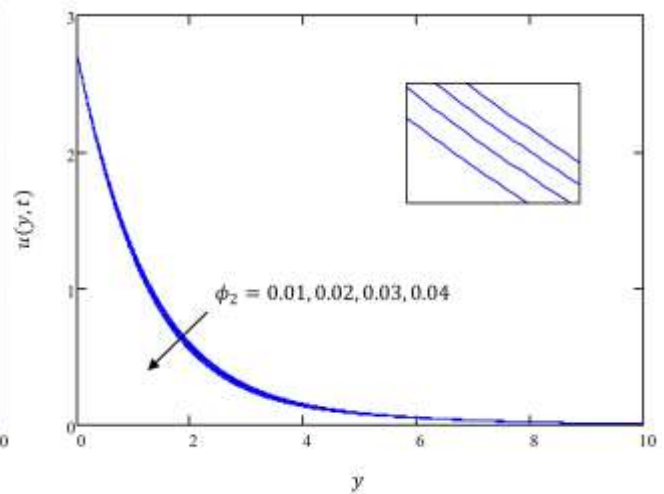
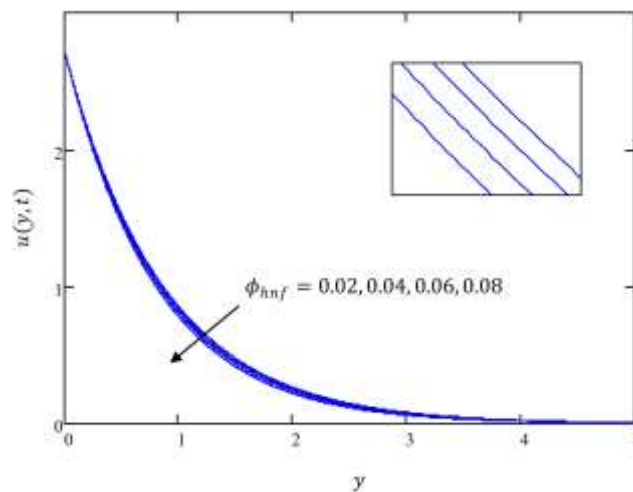**Fig. 8.** Jeffrey hybrid nanofluid velocity, $u(y,t)$ vs volume fraction of Cu, ϕ_2

Fig. 9. Jeffrey hybrid nanofluid velocity, $u(y,t)$ vs volume fraction of hybrid nanoparticle, ϕ_{hnf}

Figure 10 illustrates the impact of various base fluid types which are water ($\Pr = 6.2$), kerosene ($\Pr = 21$), and ethylene glycols ($\Pr = 203$), showing directly the effect of different Pr values on velocity profiles. The Prandtl number essentially compares the rate of momentum diffusion (viscous effects) to the rate of thermal diffusion (heat conduction) in the fluid. Higher Prandtl numbers indicate that viscosity dominates within the fluid. This means that as the Pr increases, the velocity profile decreases, and the momentum boundary layer becomes thinner due to higher fluid viscosity. According to this analysis, water has the highest velocity, followed by kerosene and ethylene glycol. Therefore, it can be inferred that water has the lowest Prandtl number among these fluids, resulting in the lowest viscosity and thus the highest velocity. In heat exchangers, this finding potentially reduces heat transfer rates. This would require adjustments in system design, such as increasing surface area or optimizing flow rates, to maintain efficient thermal performance. In biomedical devices like cooling systems for medical equipment or blood flow simulation devices, this finding

affects the device's ability to regulate temperature effectively. To ensure proper function, the fluid properties or operating conditions may need to be modified.

Physically, the Pr does not directly affect the velocity profile in the same way it affects the temperature profile. The Pr is more directly related to the thermal properties of the fluid rather than its momentum properties. However, there can be indirect effects on the velocity profile due to changes in the temperature distribution and associated buoyancy effects, particularly in situations involving natural convection or buoyancy-driven flows. It is important to note that the fluid motion in this current problem is driven by buoyancy forces (natural convection). Therefore, the steeper temperature gradients resulting from increasing Pr values will enhance the buoyancy forces locally, potentially increasing the velocity profiles.

Next, Figure 11 illustrates the difference in velocity profiles for water without nanoparticles effect (convectional Jeffrey fluid), water with separately suspended Al_2O_3 and Cu nanoparticles (Jeffrey nanofluids), and water with suspended both Al_2O_3 and Cu nanoparticles (Jeffrey hybrid nanofluid). According to the figure, water exhibits lowest viscosity compared to nanofluids and hybrid nanofluids. As a result, the velocity profile tends to be highest, with fluid particles experiencing less resistance to flow. The decrement of the velocity profile is exhibited when the fluid is influenced by nanoparticles, with the velocity decrement being more pronounced for nanofluid and hybrid nanofluid. In the case of nanofluid, water with the suspension of Al_2O_3 has a higher velocity compared to the suspension of Cu. This is due to the density of Al_2O_3 being less than the density of Cu, resulting in a less dense nanofluid that collectively impedes fluid motion and decreases flow velocities.
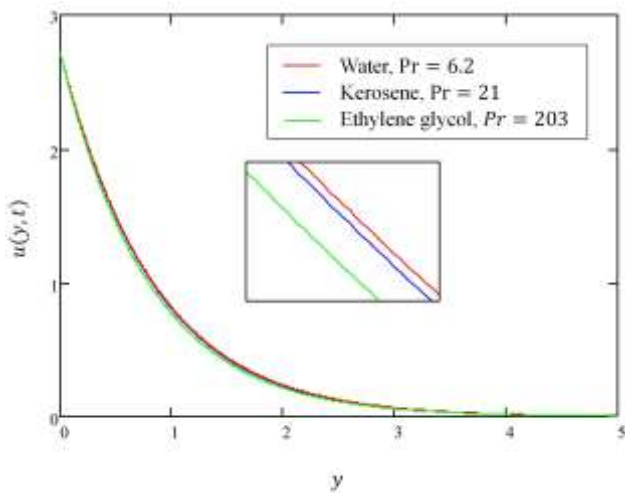

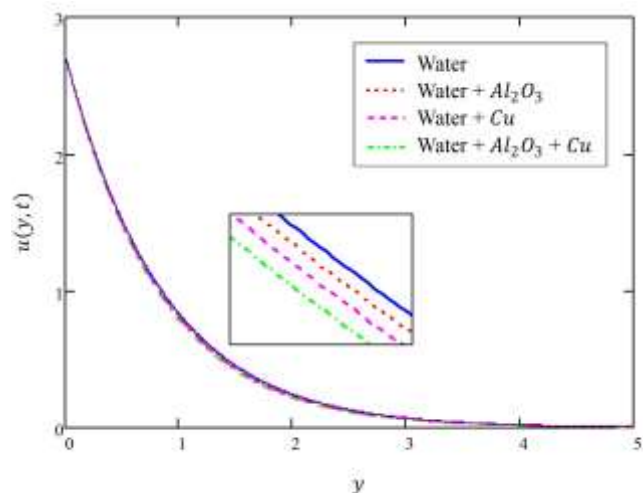**Fig. 10.** Jeffrey hybrid nanofluid velocity, $u(y,t)$ with different base fluid (Prandtl number), Pr

Fig. 11. Velocity comparison of Jeffrey hybrid nanofluid (water $+ Al_2O_3 + Cu$), Jeffrey nanofluids (water $+ Cu$ & water $+ Al_2O_3$), and conventional Jeffrey fluid (water)

Figure 12 shows the nanofluid velocity profile under the effect of magnetic field, M. The presence of magnetic field influences the behavior of the electrically conducting fluid (Jeffrey hybrid nanofluid). The motion of this fluid in a magnetic field can lead to the arise of the Lorentz force, known as the magnetohydrodynamics (MHD) phenomenon. When the strength of the magnetic field increases in a fluid flow scenario, it tends to exert a greater influence on the behavior of the fluid. An increase in the magnetic field strength results in a stronger Lorentz force acting on the fluid. This force interacts with the electric currents within the fluid, causing them to experience a greater deviation from their original path. Consequently, the fluid particles encounter more resistance to

their movement, slowing down their overall velocity. In heat exchangers, a reduced fluid velocity caused by a stronger magnetic field can lower heat transfer rates, requiring adjustments in flow rates or magnetic field strength to maintain system efficiency. In biomedical devices, such as magnetic drug targeting systems or blood pumps, increased magnetic field strength can slow fluid flow, affecting the delivery rate or circulation control.

Figure 13 illustrates the effect of porosity parameter, K on nanofluid velocity profile. The porosity parameter is investigated when the fluid is considered to flow in a porous medium. A porous medium is a material containing pores through which fluid can flow, and the porosity defines the fraction of total volume of the medium that is occupied by pores. When the porosity of a medium through which a fluid flows increases, it generally has the effect of augmenting the velocity profile of the fluid. Greater porosity often corresponds to improved permeability of the medium. Permeability measures the ease with which fluids can move through a porous material. With increased porosity, the medium becomes more permeable, allowing fluid to penetrate and propagate through the medium more readily, thereby increasing the velocity profile. In heat exchangers, this result enhances heat transfer efficiency. This could lead to more effective designs for porous heat exchangers, where maximizing fluid penetration improves thermal performance. In biomedical devices, such as filtration systems or porous implants, higher porosity allows for better fluid transport, improving circulation and delivery of drugs or nutrients. For example, in tissue engineering, optimizing the porosity of scaffolds could improve nutrient flow, aiding in tissue regeneration.
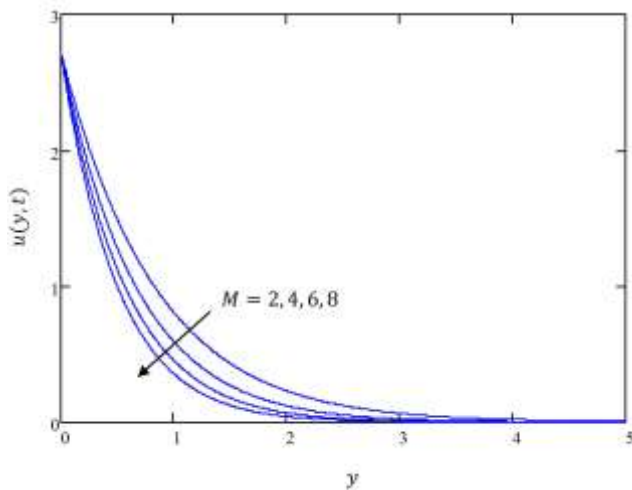

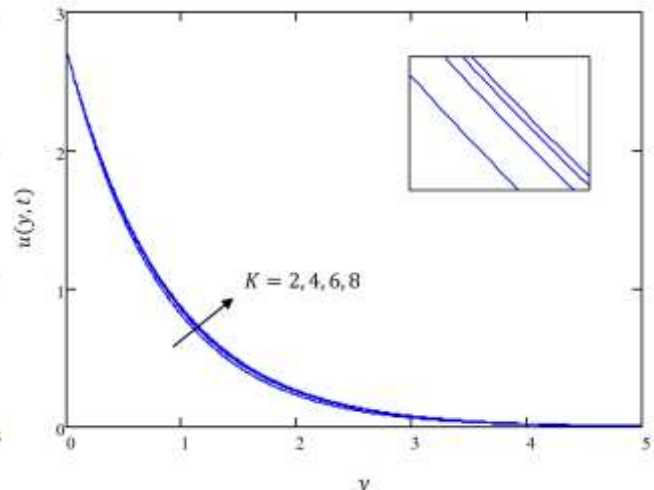**Fig. 12.** Jeffrey hybrid nanofluid velocity, $u(y,t)$ vs magnetic field, M

Fig. 13. Jeffrey hybrid nanofluid velocity, $u(y,t)$ vs porosity parameter, K

The influence of radiation parameter, Rd on the nanofluid velocity profile is depicted in Figure 14. When radiation levels increase, more energy is transferred to the fluid and its surroundings. This additional energy can lead to localized heating of the fluid, causing it to expand and decrease in density. In turn, the decreased density can lead to buoyancy-driven flows, which can enhance fluid mixing and increase the overall velocity profile, particularly in regions where the fluid is heated by radiation. In heat exchangers, this finding could be beneficial in systems where radiation is a key factor, such as solar thermal collectors, requiring design optimizations to leverage enhanced velocity for better heat exchange. In biomedical devices, such as hyperthermia treatments or thermal therapies, increased radiation can lead to localized heating and improved fluid circulation, aiding in more effective treatment delivery. Figure 15 presents the effects of Newtonian heating, γ on velocity profiles, where increments in γ cause the velocity to increase. Additionally, the figure demonstrates

that the hybrid nanofluid exhibits the lowest velocity profile when the Newtonian heating effect is absent ($\gamma = 0$). When the Newtonian heating effect is applied ($\gamma = 1, 2, 3$), the velocity profile is enhanced. Newtonian heating, γ, leads to localized temperature increases within the fluid, causing it to expand and decrease in density. This decrease in density can induce buoyancy-driven flows, such as natural convection, where warmer, less dense fluid rises and cooler, denser fluid sinks. This convective motion enhances fluid mixing and can increase the overall velocity profile, particularly in regions where heating is concentrated. Moreover, it is also observed that when the value of γ is greater, the velocity difference become prominent, and the boundary layer thickens. This situation shows that the velocity of hybrid nanofluid with greater γ needs a longer time to vanish and achieve a steady state slower that small γ values. In heat exchangers, the increase fluid velocity by γ enhances convective heat transfer. This could lead to more efficient thermal management, enabling systems to transfer heat faster and operate more effectively. In biomedical devices, such as blood pumps or targeted thermal treatments, Newtonian heating can improve fluid circulation and heat distribution. For instance, in hyperthermia treatments, controlling the heating effect can enhance the flow of treated fluids, increasing therapeutic effectiveness.
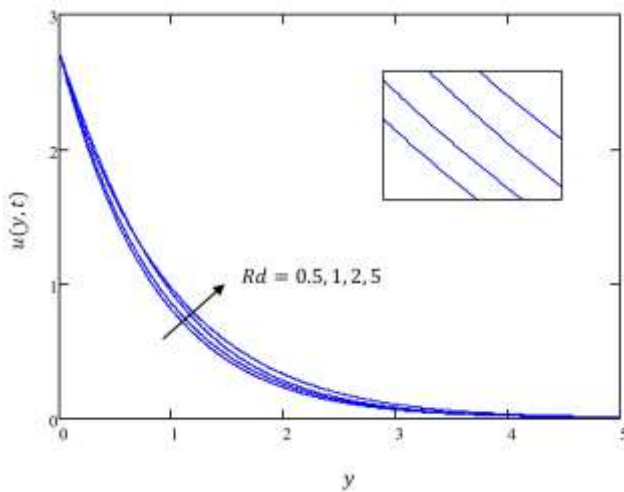

Fig. 14. Jeffrey hybrid nanofluid velocity, $u(y,t)$ vs radiation parameter, Rd
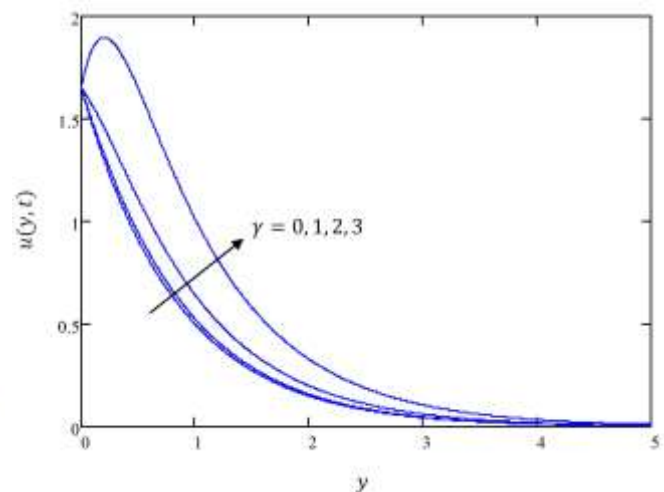
Fig. 15. Jeffrey hybrid nanofluid velocity, $u(y,t)$ vs Newtonian heating, γ

In Figure 16, the impact of Grashof number, Gr on the velocity profile is depicted. The Grashof number, Gr is a dimensionless quantity in fluid dynamics that is significant in the study of buoyancy-driven flow, particularly natural convection. It quantifies the relative significance of buoyant forces compared to viscous forces within a fluid. A higher Gr leads to an increase in the velocity profile, indicating that the buoyancy force becomes more prominent in the system when the value of Gr is higher. This dominance of buoyancy force causes the velocity profile to elevate, opposing the direction of motion. An escalation in buoyancy force propels fluid movement, thereby augmenting fluid velocity. In heat exchangers, stronger buoyancy forces can enhance natural convection, improving heat transfer efficiency by promoting fluid movement without requiring additional mechanical pumping. This can be particularly advantageous in systems where minimizing energy consumption is a priority, such as passive cooling systems or solar-powered heat exchangers. In biomedical devices, such as ventilators or fluid transport systems, enhanced buoyancy-driven flow could improve circulation in regions requiring heat dissipation or targeted cooling, as seen in hyperthermia treatments. In Figure 17, increasing values of acceleration parameter, a indicates a greater imposed velocity. The accelerated plate facilitates a more efficient flow of the nanofluid and

promotes boundary layer development. The interplay between the Gr and plate movement is crucial for enhancing heat transfer processes in various applications such as thermal exchangers, cooling systems, electronic components, and aerospace engineering.
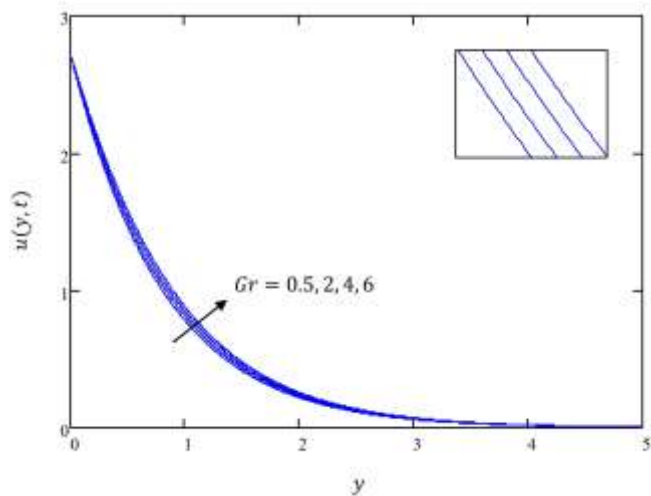

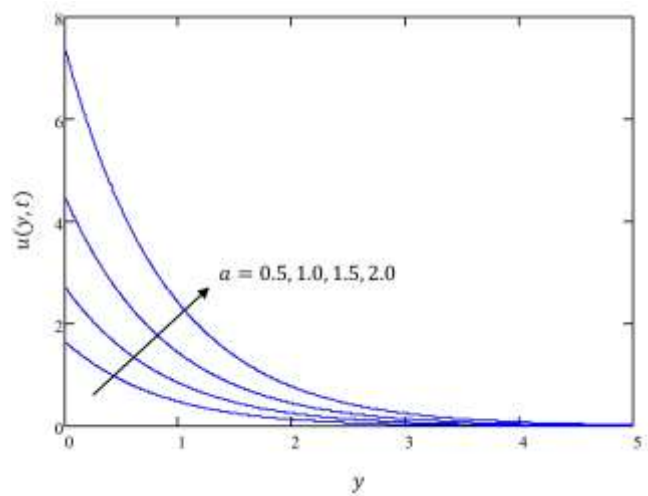**Fig. 16.** Jeffrey hybrid nanofluid velocity, $u(y,t)$ vs Garshof number, Gr

Fig. 17. Jeffrey hybrid nanofluid velocity, $u(y,t)$ vs acceleration parameter, a

4.3 Temperature Profiles

The results of increment Al_2O_3 volume fraction, ϕ_1 and Cu volume fraction, ϕ_2 on temperature profiles are shown in Figure 18 and 19, where growing temperature profiles for both types of nanoparticles are observed. Nanoparticles typically have higher thermal conductivities compared to the base fluid. As the ϕ_1 and ϕ_2 increase, the overall thermal conductivity of the hybrid nanofluid also increases. This allows for more efficient heat transfer within the fluid, leading to a higher temperature profile throughout the system. In addition, increasing volume fraction of hybrid nanofluid, ϕ_{hnf} also exhibits the same results as increasing ϕ_1 and ϕ_2, facilitating faster heat transfer and leading to an elevated temperature profile as in Figure 20. In heat exchangers, this could enable the design of more compact and efficient systems by utilizing higher ϕ_{hnf} values to achieve faster temperature regulation, especially in high-performance cooling applications like electronics or industrial processes. In biomedical devices, such as drug delivery systems or thermal therapies, increasing ϕ_{hnf} can improve the control of localized heat distribution, enhancing the efficacy of treatments like hyperthermia. In this analysis, water is used as the base fluid to suspend the hybrid nanoparticles. Based on Figure 21, the temperature difference between water ($\text{Pr} = 6.2$), kerosene ($\text{Pr} = 21$), and ethylene glycol ($\text{Pr} = 203$) is demonstrated, showing that water has the highest temperature profile and followed by kerosene and ethylene glycol. The Prandtl number, Pr is the ratio of momentum diffusivity to thermal diffusivity. A higher Pr indicates that thermal diffusivity is relatively lower compared to momentum diffusivity. This means that heat transfers more slowly compared to momentum within the fluid. As a result, increasing the Pr reduces the rate of heat transfer away from hot regions, leading to a decrease in temperature throughout the fluid and a flatter temperature profile.
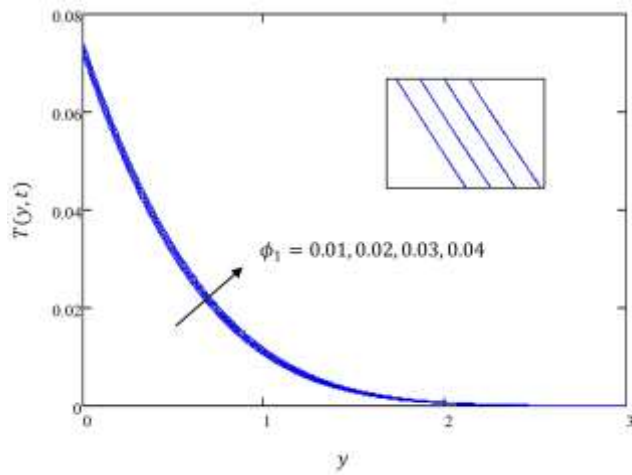
Fig. 18. Jeffrey hybrid nanofluid temperature, $T(y,t)$ vs volume fraction of Al_2O_3, ϕ_1
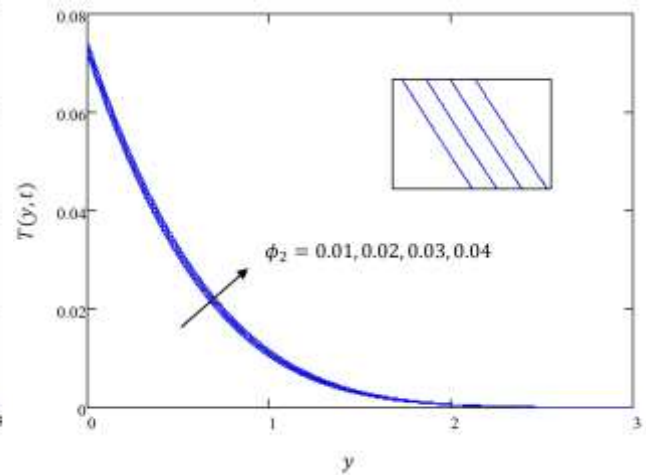

Fig. 19. Jeffrey hybrid nanofluid temperature, $T(y,t)$ vs volume fraction of Cu, ϕ_2
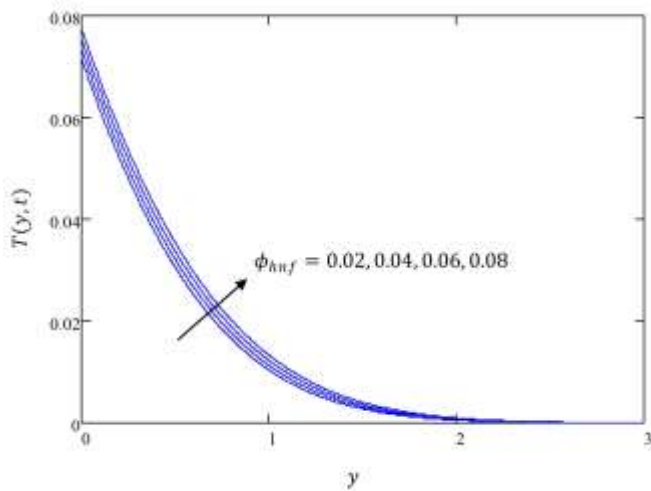

Fig. 20. Jeffrey hybrid nanofluid temperature, $T(y,t)$ vs volume fraction of hybrid nanoparticles ϕ_{hnf}
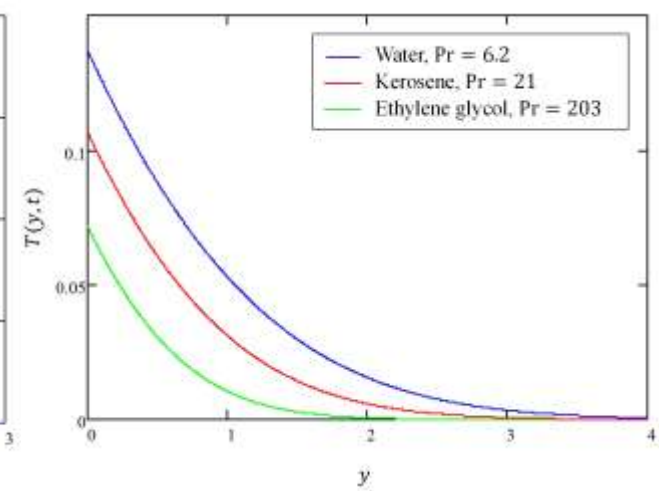

Fig. 21. Jeffrey hybrid nanofluid temperature, $T(y,t)$ with different base fluid (Prandtl number), Pr

The effect of radiation, Rd on temperature profile is illustrated in Figure 22, where an increasing trend is reported when radiation level is increased. As the radiation effect intensifies, the fluid absorbs more radiant energy. This absorbed energy increases the internal energy of the fluid, resulting in a higher temperature. Next, Figure 23 demonstrates the influences of Newtonian heating, γ on temperature profile. As the value of γ increases, the heat profile also rises. Without Newtonian heating ($\gamma = 0$), the hybrid nanofluid exhibits the lowest temperature profile, whereas the presence of Newtonian heating ($\gamma = 0.1, 0.2, 0.3$) significantly increases the temperature profile. Physically, Newtonian heating refers to a situation where the heat flux on the boundary is proportional to the local temperature difference. When the Newtonian heating effect is increased, more heat is supplied directly to the fluid from the boundary. This additional heat input raises the fluid's temperature. In biomedical devices, such as hyperthermia treatments or thermal regulation systems, controlling Rd and γ can improve temperature control and heat distribution within the body. This is critical for ensuring the safe and effective delivery of heat in medical therapies, where precise temperature adjustments are necessary for therapeutic outcomes.
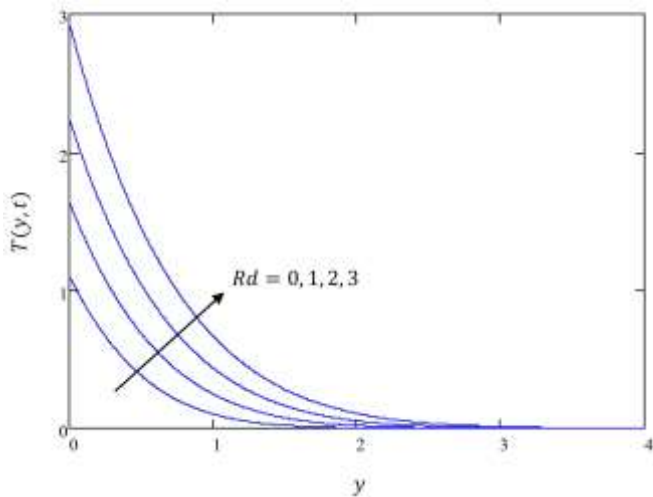
Fig. 22. Jeffrey hybrid nanofluid temperature, $T(y,t)$ vs radiation parameter, Rd
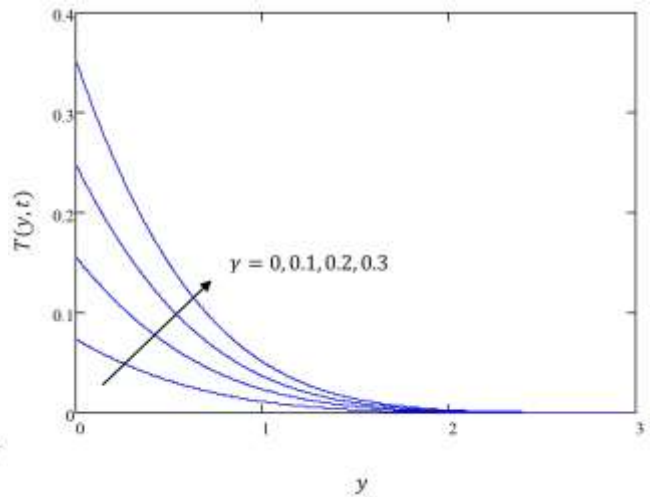
Fig. 23. Jeffrey hybrid nanofluid temperature, $T(y,t)$ vs Newtonian heating, γ

To summarize all the obtained result, the behavior of velocity and temperature profiles is tabulated in the following table, Table 3. This table provides a clear and concise understanding of complex interactions within fluid dynamics.

Table 3
Result summarization of velocity and temperature profiles

λ_1	λ	M	K	γ	Rd	Gr	a	ϕ_1	ϕ_2	ϕ_{hnf}	$u(y,t)$	$T(y,t)$
↑	1	2	2	0.5	0.5	2	1	0.01	0.01	0.02	↑	-
1	↑	2	2	0.5	0.5	2	1	0.01	0.01	0.02	↓	-
1	1	↑	2	0.5	0.5	2	1	0.01	0.01	0.02	↓	-
1	1	2	↑	0.5	0.5	2	1	0.01	0.01	0.02	↑	-
1	1	2	2	↑	0.5	2	1	0.01	0.01	0.02	↑	↑
1	1	2	2	0.5	↑	2	1	0.01	0.01	0.02	↑	↑
1	1	2	2	0.5	0.5	↑	1	0.01	0.01	0.02	↑	-
1	1	2	2	0.5	0.5	2	↑	0.01	0.01	0.02	↑	-
1	1	2	2	0.5	0.5	2	1	↑	0.01	↑	↓	↑
1	1	2	2	0.5	0.5	2	1	0.01	↑	↑	↓	↑
1	1	2	2	0.5	0.5	2	1	↑	↑	↑	↓	↑

↑	Increasing the value of parameter	↑	Increasing profile
-	Not considered	↓	Decreasing profile

5. Conclusion

This article investigates the interaction between MHD and porosity in an unsteady flow of radiative Jeffrey hybrid nanofluid under the influence of Newtonian heating. The flow of nanofluid is bounded with an exponentially accelerated plate. The analytical computation is performed with Laplace transform method. The velocity and temperature profiles under the influences of pertinent parameters are illustrated graphically. The significant findings are observed as follows:

i) An increase of ϕ_1, ϕ_2, and ϕ_{hnf} increases the viscosity of fluid and leads to a decreasing velocity profile. Meanwhile, an increase of ϕ_1, ϕ_2, and ϕ_{hnf} elevates the temperature profiles due to an enhancement of thermal conductivity.

ii) As the value of γ increases, the velocity accelerates due to less resistance to flow and the temperature increases because more absorption of heat occurred in the fluid.

iii) When Rd level is high, the fluid experiences less obstacles and cause the velocity to elevate. In addition, a growth in temperature profile is also obtained when increasing Rd because the fluid absorbs more heat.

iv) Increasing the strength of M cause the retardation of velocity due to the fluid experiences high resistance in the flow.

v) As K, Gr, and a increases, the flow produces less obstacles and the fluid velocity increases.

vi) An increasing velocity profile is exhibited for increasing λ_1 values, while decreasing velocity profile is exhibited for increasing λ values. This situation is reflected in the viscoelastic behavior of the Jeffrey fluid.

vii) The comparison of different base fluids shows that the highest velocity and temperature profile are achieved when using water as the base fluid.

Acknowledgement

References

[1] Okuyade, Ighoroje WA, and Tamunoimi M. Abbey. "Transient MHD Fluid Flow Past a Moving Vertical Surface in a Velocity Slip Flow Regime." *WSEAS Transactions on Fluid Mechanics* 19 (2024): 99-112. https://doi.org/10.37394/232013.2024.19.10

[2] Wan Azmi, Wan Faezah, Ahmad Qushairi Mohamad, Lim Yeou Jiann, and Sharidan Shafie. "Mathematical Modelling of MHD Blood Flow with Gold Nanoparticles in Slip Small Arteries." *Journal of Applied and Computational Mechanics* 10, no. 1 (2024): 125-139. https://doi.org/10.22055/jacm.2023.44057.4160

[3] Ali, Farhan, A. Zaib, M. Khalid, T. Padmavathi, and B. Hemalatha. "Unsteady MHD Flow of Casson Fluid Past Vertical Surface Using Laplace Transform Solution." *Journal of Computational Biophysics and Chemistry* 22, no. 03 (2023): 361-370. https://doi.org/10.1142/S2737416523400100

[4] Sehra, Sehra, Afshan Noor, Sami Ul Haq, Saeed Ullah Jan, Ilyas Khan, and Abdullah Mohamed. "Heat transfer of generalized second grade fluid with MHD, radiation and exponential heating using Caputo–Fabrizio fractional derivatives approach." *Scientific Reports* 13, no. 1 (2023): 5220. https://doi.org/10.1038/s41598-022-22665-4

[5] Noranuar, W. N. N., A. Qushairi Mohamad, S. Shafie, and I. Khan. "Accelerated non-coaxial rotating flow of MHD viscous fluid with heat and mass transfer." In *IOP Conference Series: Materials Science and Engineering*, vol. 1051, no. 1, p. 012044. IOP Publishing, 2021. https://doi.org/10.1088/1757-899X/1051/1/012044

[6] Ramzan, Muhammad, Ahmad Shafique, Shajar Abbas, Elsiddeg Ali, Aiedh Mrisi Alharthi, and Rashid Jan. "Effect of slip on MHD flow of fluid with heat and mass transfer through a plate." *Radiation Effects and Defects in Solids* (2024): 1-13. https://doi.org/10.1080/10420150.2024.2397137

[7] Krishna, M. Veera, M. Gangadhar Reddy, and Ali J. Chamkha. "Heat and mass transfer on unsteady MHD flow through an infinite oscillating vertical porous surface." *Journal of Porous Media* 24, no. 1 (2021). https://doi.org/10.1615/JPorMedia.2020025021

[8] Wu, Yunyun, and Jia Xu. "Simplified analysis of MHD flow in a porous surrounding bounded by an oscillating vertical cylindrical surface." *Case Studies in Thermal Engineering* 30 (2022): 101737. https://doi.org/10.1016/j.csite.2021.101737

[9] Omar, Nur Fatihah Mod, Husna Izzati Osman, Ahmad Qushairi Mohamad, Rahimah Jusoh, and Zulkhibri Ismail. "Analytical solution of unsteady MHD Casson fluid with thermal radiation and chemical reaction in porous medium." *Journal of Advanced Research in Applied Sciences and Engineering Technology* 29, no. 2 (2023): 185-194. https://doi.org/10.37934/araset.29.2.185194

[10] Noranuar, Wan Nura'in Nabilah, Ahmad Qushairi Mohamad, Sharidan Shafie, and Lim Yeou Jiann. "Heat and mass transfer on Magnetohydrodynamics Casson carbon nanotubes nanofluid flow in an asymmetrical channel via porous medium." *Symmetry* 15, no. 4 (2023): 946. https://doi.org/10.3390/sym15040946

[11] Haq, Sami Ul, Hammad Khaliq, Saeed Ullah Jan, Aisha M. Alqahtani, Ilyas Khan, and Md Nur Alam. "General solution for unsteady MHD natural convection flow with arbitrary motion of the infinite vertical plate embedded in porous medium." *Journal of Mathematics* 2022, no. 1 (2022): 9959564. https://doi.org/10.1155/2022/9959564

[12] Abbas, Shajar, Zaib Un Nisa, Mudassar Nazar, Ahmed Sayed M. Metwally, Krzysztof Kędzia, Ahmed Zubair Jan, and Nargiza Kamolova. "Effect of chemical reaction on MHD Casson natural convection flow over an oscillating plate in porous media using Caputo fractional derivative." *International Journal of Thermal Sciences* 207 (2025): 109355. https://doi.org/10.1016/j.ijthermalsci.2024.109355

[13] Yasin, Siti Hanani Mat, Muhammad Khairul Anuar Mohamed, Zulkhibri Ismail, Basuki Widodo, and Mohd Zuki Salleh. "Numerical solution on MHD stagnation point flow in ferrofluid with Newtonian heating and thermal radiation effect." *Journal of Advanced Research in Fluid Mechanics and Thermal Sciences* 57, no. 1 (2019): 12-22. Retrieved from https://semarakilmu.com.my/journals/index.php/fluid_mechanics_thermal_sciences/article/view/3111

[14] Puzi, Nurwardah Mohd, Mashitah Aziz, Nur Syazana Anuar, Norfifah Bachok, and Ioan Pop. "Newtonian Heating in Magnetohydrodynamic (MHD) Hybrid Nanofluid Flow Near the Stagnation Point over Nonlinear Stretching and Shrinking Sheet." *Journal of Advanced Research in Numerical Heat Transfer* 20, no. 1 (2024): 53-67. https://doi.org/10.37934/arnht.20.1.5367

[15] Aleem, Maryam, Muhammad Imran Asjad, Aqila Shaheen, and Ilyas Khan. "MHD Influence on different water based nanofluids (TiO2, Al2O3, CuO) in porous medium with chemical reaction and newtonian heating." *Chaos, Solitons & Fractals* 130 (2020): 109437. https://doi.org/10.1016/j.chaos.2019.109437

[16] Riaz, Muhammad Bilal, Jan Awrejcewicz, and Dumitru Baleanu. "Exact solutions for thermomagetized unsteady non-singularized jeffrey fluid: Effects of ramped velocity, concentration with newtonian heating." *Results in physics* 26 (2021): 104367. https://doi.org/10.1016/j.rinp.2021.104367

[17] Mohd Zin, Nor Athirah, Ilyas Khan, and Sharidan Shafie. "Exact and numerical solutions for unsteady heat and mass transfer problem of Jeffrey fluid with MHD and Newtonian heating effects." *Neural Computing and Applications* 30, no. 11 (2018): 3491-3507. https://doi.org/10.1007/s00521-017-2935-6

[18] Ramzan, M., A. Shafique, M. Amir, M. Nazar, and Zaib Un Nisa. "MHD flow of fractionalized Jeffrey fluid with Newtonian heating and thermal radiationover a vertical plate." *International Journal of Sciences: Basic and Applied Research* 61 (2022): 170-195.

[19] Anwar, Talha, Poom Kumam, Ilyas Khan, and Phatiphat Thounthong. "Generalized unsteady MHD natural convective flow of Jeffery model with ramped wall velocity and Newtonian heating; a Caputo-Fabrizio approach." *Chinese Journal of Physics* 68 (2020): 849-865. https://doi.org/10.1016/j.cjph.2020.10.018

[20] Ishtiaq, Fehid, Rahmat Ellahi, Muhammad Mubashir Bhatti, and Sultan Z. Alamri. "Insight in thermally radiative cilia-driven flow of electrically conducting non-Newtonian Jeffrey fluid under the influence of induced magnetic field." *Mathematics* 10, no. 12 (2022): 2007. https://doi.org/10.3390/math10122007

[21] Akbar, Noreen Sher, S. Nadeem, and Mohamed Ali. "Jeffrey fluid model for blood flow through a tapered artery with a stenosis." *Journal of Mechanics in Medicine and Biology* 11, no. 03 (2011): 529-545. https://doi.org/10.1142/S0219519411003879

[22] Zin, Nor Athirah Mohd, Ilyas Khan, Sharidan Shafie, and Ali Saleh Alshomrani. "Analysis of heat transfer for unsteady MHD free convection flow of rotating Jeffrey nanofluid saturated in a porous medium." *Results in physics* 7 (2017): 288-309. https://doi.org/10.1016/j.rinp.2016.12.032

[23] Hari Babu, B., P. Srinivasa Rao, and S. V. K. Varma. "Hall and ion-slip effects on MHD free convection flow of rotating Jeffrey fluid over an infinite vertical porous surface." *Heat Transfer* 50, no. 2 (2021): 1776-1798. https://doi.org/10.1002/htj.21954

[24] Krishna, M. Veera. "Hall and ion slip effects on radiative MHD rotating flow of Jeffreys fluid past an infinite vertical flat porous surface with ramped wall velocity and temperature." *International communications in Heat and Mass transfer* 126 (2021): 105399. https://doi.org/10.1016/j.icheatmasstransfer.2021.105399

[25] Asjad, Muhammad Imran, Abdul Basit, Ali Akgül, and Taseer Muhammad. "Generalized thermal flux flow for Jeffrey fluid with fourier law over an infinite plate." *Mathematical Problems in Engineering* 2021, no. 1 (2021): 5403879. https://doi.org/10.1155/2021/5403879

[26] Bajwa, Sana, Saif Ullah, Amnah S. Al-Johani, Ilyas Khan, and Mulugeta Andualem. "Effects of MHD and porosity on Jeffrey fluid flow with wall transpiration." *Mathematical Problems in Engineering* 2022, no. 1 (2022): 6063143. https://doi.org/10.1155/2022/6063143

[27] Aleem, Maryam, Muhammad Imran Asjad, Ali Ahmadian, Mehdi Salimi, and Massimiano Ferrara. "Heat transfer analysis of channel flow of MHD Jeffrey fluid subject to generalized boundary conditions." *The European physical journal plus* 135, no. 1 (2020): 26. https://doi.org/10.1140/epjp/s13360-019-00071-6

[28] Siddique, Imran, Rubina Adrees, Hijaz Ahmad, and Sameh Askar. "MHD free convection flows of Jeffrey fluid with Prabhakar-like fractional model subject to generalized thermal transport." *Scientific Reports* 13, no. 1 (2023): 9289. https://doi.org/10.1038/s41598-023-36436-2

[29] Mohamed, Hozaifa A., Majed Alhazmy, F. Mansour, and El-Sayed R. Negeed. "Heat transfer enhancement using CuO nanofluid in a double pipe U-bend heat exchanger." *Journal of Nanofluids* 12, no. 5 (2023): 1260-1274. https://doi.org/10.1166/jon.2023.2014

[30] Memet, Feiza. "Heat transfer analysis when using Al2O3–water nanofluid in a double pipe heat exchanger with parallel flow arrangement." In *Advanced Topics in Optoelectronics, Microelectronics, and Nanotechnologies XI*, vol. 12493, pp. 81-86. SPIE, 2023. https://doi.org/10.1117/12.2642034

[31] Kumar, Sunil, Mridul Sharma, Anju Bala, Anil Kumar, Rajesh Maithani, Sachin Sharma, Tabish Alam, Naveen Kumar Gupta, and Mohsen Sharifpur. "Enhanced heat transfer using oil-based nanofluid flow through Conduits: A Review." *Energies* 15, no. 22 (2022): 8422. https://doi.org/10.3390/en15228422

[32] Elfaghi, Abdulhafid MA, Alhadi A. Abosbaia, Munir FA Alkbir, and Abdoulhdi AB Omran. "Heat transfer enhancement in pipe using Al2O3/water nanofluid." *CFD Letters* 14, no. 9 (2022): 118-124. https://doi.org/10.37934/cfdl.14.9.118124

[33] Suresh, Sivan, K. P. Venkitaraj, Ponnusamy Selvakumar, and Murugesan Chandrasekar. "Effect of Al2O3–Cu/water hybrid nanofluid in heat transfer." *Experimental Thermal and Fluid Science* 38 (2012): 54-60. https://doi.org/10.1016/j.expthermflusci.2011.11.007

[34] Waini, Iskandar, Anuar Ishak, Teodor Groşan, and Ioan Pop. "Mixed convection of a hybrid nanofluid flow along a vertical surface embedded in a porous medium." *International Communications in Heat and Mass Transfer* 114 (2020): 104565. https://doi.org/10.1016/j.icheatmasstransfer.2020.104565

[35] Eshgarf, Hamed, Rasool Kalbasi, Akbar Maleki, Mostafa Safdari Shadloo, and Arash Karimipour. "A review on the properties, preparation, models and stability of hybrid nanofluids to optimize energy consumption." *Journal of Thermal Analysis and Calorimetry* 144 (2021): 1959-1983. https://doi.org/10.1007/s10973-020-09998-w

[36] Saqib, Muhammad, Ilyas Khan, and Sharidan Shafie. "Application of fractional differential equations to heat transfer in hybrid nanofluid: modeling and solution via integral transforms." *Advances in Difference Equations* 2019, no. 1 (2019): 1-18. https://doi.org/10.1186/s13662-019-1988-5

[37] Ikram, Muhammad Danish, Muhammad Imran Asjad, Ali Akgül, and Dumitru Baleanu. "Effects of hybrid nanofluid on novel fractional model of heat transfer flow between two parallel plates." *Alexandria Engineering Journal* 60, no. 4 (2021): 3593-3604. https://doi.org/10.1016/j.aej.2021.01.054

[38] Roy, Nepal Chandra, and Ioan Pop. "Exact solutions of Stokes' second problem for hybrid nanofluid flow with a heat source." *Physics of Fluids* 33, no. 6 (2021). https://doi.org/10.1063/5.0054576

[39] Elelamy, Asmaa F. "Laser Effects on Bioheat Transfer with Non-Newtonian Hybird Nanofluid Flow: Analytical Method with Finite Sine and Laplace Transforms." *Journal of Nanofluids* 12, no. 5 (2023): 1224-1232. https://doi.org/10.1166/jon.2023.2011

[40] Rajesh, Vemula, Hakan F. Öztop, and Nidal H. Abu-Hamdeh. "Impact of moving/exponentially accelerated vertical plate on unsteady flow and heat transfer in hybrid nanofluids." *Journal of Nanofluids* 12, no. 5 (2023): 1374-1382. https://doi.org/10.1166/jon.2023.2023

[41] Anwar, Talha, and Poom Kumam. "A fractal fractional model for thermal analysis of GO– NaAlg– Gr hybrid nanofluid flow in a channel considering shape effects." *Case Studies in Thermal Engineering* 31 (2022): 101828. https://doi.org/10.1016/j.csite.2022.101828

[42] Ali, Rizwan, Muhammad Imran Asjad, Ali Aldalbahi, Mohammad Rahimi-Gorji, and Mostafizur Rahaman. "Convective flow of a Maxwell hybrid nanofluid due to pressure gradient in a channel." *Journal of Thermal Analysis and Calorimetry* 143 (2021): 1319-1329. https://doi.org/10.1007/s10973-020-10304-x

[43] Zin, Nor Athirah Mohd, Siti Nur Alwani Salleh, Ahmad Qushairi Mohamad, Mohd Rijal Ilias, and Ilyas Khan. "Heat Transfer in Hartmann Flow of Hybrid Nano-Jeffrey Fluid with Heat Absorption and Thermal Radiation Impact." *Journal of Advanced Research in Fluid Mechanics and Thermal Sciences* 112, no. 1 (2023): 38-61. https://doi.org/10.37934/arfmts.112.1.3861

[44] Wang, Liqiu, Xuesheng Zhou, and Xiaohao Wei. *Heat conduction: mathematical models and analytical solutions*. Springer Science & Business Media, 2007. https://doi.org/10.1007/978-3-540-74303-3

[45] Kato, Sumio, and Shoichi Matsuda. "Analytical solution for the problem of one-dimensional quasi-steady non-charring ablation in a semi-infinite solid with temperature-dependent thermo-physical properties." *Thermal Science and Engineering Progress* 31 (2022): 101181. https://doi.org/10.1016/j.tsep.2021.101181

[46] Kucherenko, P. A., and S. V. Sokolov. "Analytical solution for a problem on approximation of functional dependences for parameters of a geodesic line." *Mechanics of Solids* 54, no. 7 (2019): 1076-1082. https://doi.org/10.3103/S0025654419070082